J Breast Cancer. 2023 Dec;26(6):525-543
https://doi.org/10.4048/jbc.2023.26.e47
pISSN 1738-6756·eISSN 2092-9900

Journal of Breast Cancer JBC

Original Article



# Characterization of Expression and Function of the Formins FHOD1, INF2, and DAAM1 in HER2-Positive Breast Cancer

**Minna Peippo** [1,2], **Maria Gardberg** [1], **Pauliina Kronqvist** [1], **Olli Carpén** [1,2,3], **Vanina D. Heuser** [2]

[1]Department of Pathology, Turku University Hospital, University of Turku, Turku, Finland
[2]Institute of Biomedicine and FICAN West Cancer Centre, University of Turku, Turku, Finland
[3]Department of Pathology, Helsinki University Hospital, University of Helsinki, Helsinki, Finland



**Received:** Dec 31, 2022
**Revised:** Aug 31, 2023
**Accepted:** Oct 16, 2023
**Published online:** Nov 13, 2023

**Correspondence to**
**Vanina D. Heuser**
Institute of Biomedicine and FICAN West Cancer Centre, University of Turku, Medicina D5, 5th floor, room D5046, Kiinamyllynkatu 10, Turku 20520, Finland.
Email: vanheu@utu.fi



**ORCID iDs**
Minna Peippo
https://orcid.org/0000-0001-6487-6106
Maria Gardberg
https://orcid.org/0000-0002-2179-4271
Pauliina Kronqvist
https://orcid.org/0000-0001-8922-0648
Olli Carpén
https://orcid.org/0000-0002-7847-5706
Vanina D. Heuser
https://orcid.org/0000-0002-7044-4649

**Funding**
This study was supported by Medicinska Understödsföreningen Liv och Hälsa, the Finska Läkaresällskapet, the Perklén

## ABSTRACT

**Purpose:** Human epidermal growth factor receptor 2 (HER2)-targeted therapies, such as trastuzumab, benefit patients with HER2-positive metastatic breast cancer; however, owing to traditional pathway activation or alternative signaling, resistance persists. Given the crucial role of the formin family in shaping the actin cytoskeleton during cancer progression, these proteins may function downstream of the HER2 signaling pathway. Our aim was to uncover the potential correlations between formins and HER2 expression using a combination of public databases, immunohistochemistry, and functional *in vitro* assays.
**Methods:** Using online databases, we identified a negative prognostic correlation between specific formins mRNA expression in HER2-positive cancers. To validate these findings at the protein level, immunohistochemistry was performed on HER2 subtype breast cancer tumors to establish the links between staining patterns and clinical characteristics. We then knocked down individual or combined formins in MDA-MB-453 and SK-BR-3 cells and investigated their effects on wound healing, transwell migration, and proliferation. Furthermore, we investigated the effects of erb-b2 receptor tyrosine kinase 2 (ERBB2)/HER2 small interfering RNA (siRNA)-mediated knockdown on the PI3K/Akt and MEK/ERK1 pathways as well as on selected formins.
**Results:** Our results revealed that correlations between *INF2*, *FHOD1*, and *DAAM1* mRNA expression and *ERBB2* in HER2-subtype breast cancer were associated with worse outcomes. Using immunohistochemistry, we found that high FHOD1 protein expression was linked to higher histological grades and was negatively correlated with estrogen and progesterone receptor positivity. Upon formins knockdown, we observed effects on wound healing and transwell migration, with a minimal impact on proliferation, which was evident through single and combined knockdowns in both cell lines. Notably, siRNA-mediated knockdown of HER2 affected FHOD1 and INF2 expression, along with the phosphorylated Akt/MAPK states.
**Conclusion:** Our study highlights the roles of FHOD1 and INF2 as downstream effectors of the HER2/Akt and HER2/MAPK pathways, suggesting that they are potential therapeutic targets in HER2-positive breast cancer.

**Keywords:** Breast Neoplasms; Cytoskeletal Proteins; Formins; Receptor, ErbB-2; Signal Transduction

foundation, the Cancer Societies of Southwest Finland, and Turku University Hospital Research Funds.

**Conflict of Interest**

The authors declare that they have no competing interests.

**Data Availability**

In accordance with the ICMJE data sharing policy, the authors have agreed to make the data available upon request.

**Author Contributions**

Conceptualization: Peippo M, Gardberg M, Carpén O, Heuser VD; Data curation: Kronqvist P; Formal analysis: Peippo M, Gardberg M, Heuser VD; Funding acquisition: Carpén O, Gardberg M; Investigation: Peippo M, Gardberg M, Heuser VD; Methodology: Peippo M, Gardberg M, Kronqvist P, Heuser VD; Project administration: Heuser VD; Resources: Carpén O; Supervision: Carpén O, Heuser VD; Writing - original draft: Heuser VD; Writing - review & editing: Peippo M, Gardberg M, Kronqvist P, Carpén O, Heuser VD.

## INTRODUCTION

Breast cancer, with an estimated 2.3 million new cases annually, was the predominant contributor to global cancer incidence in 2020, constituting 11.7% of all cancer cases. Despite advancements in treatments that have yielded improved prognoses, the prevalence of metastatic breast cancer remains a significant contributor to cancer-related mortality, accounting for approximately 685,000 deaths annually [1]. Molecularly classified by surrogate markers, breast cancer can be categorized into four primary subtypes dependent on the presence of estrogen or progesterone receptors (ER and PgR) and amplification of the human epidermal growth factor receptor 2/erb-b2 receptor tyrosine kinase 2 (HER2/ERBB2) gene [2].

HER2/ERBB2 belongs to the epidermal growth factor (EGF) receptor family of receptor tyrosine kinases, comprising three additional members: EGFR, HER1, and HER3 (encoded by the *ERBB1*, *ERBB3*, and *ERBB4* genes, respectively). Family members can form either heterodimers or homodimers. Among the various dimer combinations, the HER2/HER3 heterodimer is the most potent oncogenic pairing, leading to the robust stimulation of the PI3K/Akt pathway. This combination is particularly important for HER2-mediated signaling in tumors with *ERBB2* amplification [3]. Other intracellular signaling pathways downstream of HER2 include MEK/MAPK, JAK/STAT3, PLC/PKC, and Src [4]. These critical signaling cascades play crucial roles in governing essential cellular processes such as proliferation, migration, differentiation, motility, and apoptosis.

Elevated HER2/ERBB2 expression is linked to early tumor dissemination and unfavorable clinical outcomes if not addressed by HER2-targeted therapies [5], including anti-HER2 antibodies (e.g., trastuzumab and pertuzumab) and small-molecule tyrosine kinase inhibitors (such as lapatinib and neratinib). Although many patients with HER2-positive metastatic breast cancer benefit from trastuzumab-containing therapy, many still experience disease progression due to traditional pathway activation or alternative signaling.

During cancer progression, the complex actions of cell invasion and migration rely on dynamic changes in the cell cytoskeleton. This leads to the formation of different membrane protrusions such as ruffles, lamellipodia, filopodia, and invadopodia. The formin family of actin nucleators is involved in actin cytoskeleton remodeling. Comprising a total of fifteen distinct proteins [6], the formin family encompasses a diverse array of actin-rearranging activities, coupled with expression profiles that vary depending on the specific cell type. These individual formins are involved in the migration and proliferation of various cancer cell types, including leukemia [7], melanomas [8,9], triple-negative breast cancer [10], and bone metastasis [11]. Formins are upregulated in malignancies such as head and neck squamous carcinoma [12], gastric cancer [13], and pancreatic cancer [14]. In our previous studies, we determined the regulatory potential of the PI3K and/or MAPK pathways in modulating formin expression in melanoma and squamous cell carcinoma cells [8,12]. Therefore, formins are promising downstream effectors of the HER2 pathway. The identification of effector molecules that orchestrate cytoskeletal changes associated with disease progression, even after the attenuation of the effects of HER2-targeting therapy, could provide valuable insights for the development of innovative therapeutic strategies.

In the present study, we aimed to identify the association between formin and HER2 by searching for formins mRNAs correlated with *ERBB2* expression using publicly available databases. Among HER2-positive cancers, we tested whether formins mRNA expression had

a negative prognostic value. We found that three formins (*INF2, FHOD1,* and *DAAM1*) were associated with poor patient outcomes.

To validate these findings at the protein level, we conducted immunohistochemistry (IHC) analyses on a cohort of HER2 subtype breast cancer tumors. Next, we conducted cellular experiments to investigate the potential consequences of HER2/ERBB2 small interfering RNA (siRNA)-mediated knockdown on the PI3K/Akt and MEK/ERK1 pathways, along with the expression of FHOD1, INF2, and DAAM1. Furthermore, we examined the effect of suppressing each of these formins and their combinations on cell migratory and proliferative capabilities.

## METHODS

### Analysis of mRNA data from public databases

The prognostic significance of formin (all except *GRID2IP*) mRNA expression in HER2-positive breast cancers was assessed using the publicly available online database Kaplan–Meier Plotter (www.kmplot.com) [15]. The cutoff values and probe numbers are listed in **Supplementary Table 1**.

The correlations between the 14 formins and *ERBB2* mRNA expression (Log2(TPM+1)) in 230 HER2 subtype breast tumors were obtained from GENT2 (Gene Expression database of Normal and Tumor tissues), freely available at http://gent2.appex.kr [16].

### Patient samples

The study comprised a cohort of 70 patients who underwent surgery for HER2-positive subtype invasive breast carcinoma at Turku University Hospital, Turku, Finland, during the period from 2008 to 2013. Tissue microarrays (TMA) containing invasive areas from patient samples, along with clinical follow-up information obtained from pathology reports and patient records, were procured from Auria Biobank under Decision AB20-2144 and research permission T208_2020 from Hospital District of Southwest Finland. The follow-up data contained crucial prognostic indicators for breast cancer treatment. These included the HER2-oncogene status, tumor size, Ki-67 proliferation marker, ER and PgR positivity, axillary lymph node status, histological grade, and intrinsic classification. The follow-up duration ranged from 5 years and 4 months to 12 years, with an average of 9 years and 6 months.

All tissue materials were prepared according to basic clinical histopathology laboratory practices, that is, fixed in buffered formalin (pH 7.0) and embedded in paraffin. IHC was performed on TMAs comprising tissue samples from both the center and the invasive border of the tumor from each patient. The TMA was prepared by punching the paraffin block of each tumor using a 1.0-mm diameter cylinder.

### IHC

TMAs were sectioned at 3.5 μm and stained with rabbit anti-human FHOD1 (1:500; Sigma-Aldrich, USA), INF2 (1:500; Proteintech, USA), and DAAM1 (1:200; Proteintech). Immunostaining was performed according to the streptavidin-peroxidase method, using a Labvision staining device (Thermo Fisher Scientific, USA). Stained slides were scanned using a NanoZoomer S60 slide scanner (Hamamatsu Photonics, Japan), and a pathologist (MG) and researcher (MP) evaluated the staining intensity using the NDP.view2 Image viewing software (Hamamatsu).


https://doi.org/10.4048/jbc.2023.26.e47

## Cell culture

Human HER2-amplified breast cancer cell lines MDA-MB-453 and SK-BR-3 were obtained from the American Type Culture Collection (USA). The cells were maintained in Dulbecco's Modified Eagle Medium (DMEM; Lonza, Switzerland) supplemented with 10% fetal bovine serum (FBS; Lonza), 5 mM ultraglutamine, and 100 U/mL penicillin-streptomycin (Gibco, USA). The cells were grown in an incubator at 37°C with 5% $CO_2$ and periodically checked for mycoplasma contamination using a MycoAlertTM mycoplasma detection kit (Lonza).

In experiments where signaling pathways were inhibited, the cells were kept in starvation medium (DMEM 0.5% FBS) overnight and then cultured for 24 hours in a medium containing 10 μM MEK 1/2 inhibitor U0126 (Cell Signaling Technology, USA), 10 μM PI3 kinase inhibitor LY294002 (Tocris Bioscience, UK), or DMSO (Thermo Fisher Scientific) as a negative control.

## Cell immunofluorescence staining and microscopy

Cells were seeded onto 13 mm coverslips coated with 100 μg/mL gelatin (Sigma-Aldrich) and cultured in complete medium for 24 hours. Staining was performed as previously described [9]. The primary antibodies used were rabbit anti-human HER2/ErbB2 (Proteintech), FHOD1 (Sigma-Aldrich), INF2 (Proteintech), and DAAM1 (Proteintech) (all diluted 1:100). The secondary antibody was Alexa Fluor 568 goat anti-rabbit IgG (1:500; Invitrogen, USA). For the visualization of actin filaments, Alexa Fluor 488- or 568-conjugated phalloidin (1:500; Invitrogen) was incubated alone or together with the secondary antibody. The mounting medium contained 4′,6-diamidino-2-phenylindole (DAPI) for staining nuclei (ProLong® Gold Antifade Mounting with DAPI; Thermo Fisher Scientific). Images were captured using a Nikon Eclipse Ni fluorescence microscope (Nikon, Japan), and different channels were merged using the ImageJ 1.53t software (http://rsbweb.nih.gov/ij/).

## siRNA mediated knockdowns

MDA-MB-453 and SK-BR-3 cells were transfected in suspension with 15 and 5 μL/mL of Dharmafect 4 (Dharmacon Research, USA), respectively. The expression of FHOD1, INF2, and DAAM1 was individually or simultaneously suppressed using 50 nM FHOD1 siRNA (SMARTpool, Dharmacon Research), INF2, and/or DAAM1 siRNA (FlexiTube siRNA, Qiagen Sciences, USA). HER2/ERBB2 expression was knocked down using 50 nM ERBB2 FlexiTube siRNA (Qiagen). The effectiveness of knockdown was assessed 48-hour post-transfection by immunoblotting in each independent experiment.

## Western blotting

Western blot samples were collected and processed as previously described [9]. To verify the efficacy of the siRNA treatments, we used rabbit anti-HER2/ERBB2 (Proteintech), FHOD1 (Sigma-Aldrich), INF2, and DAAM1 (both Proteintech) antibodies. PI3K/Akt pathway inhibition was verified by immunoblotting using rabbit anti-pAkt and Akt antibodies (Cell Signaling Technology), and MEK/ERK pathway inhibition was verified by immunoblotting with a rabbit anti-p44/42 MAPK (Erk1/2) antibody (Cell Signaling Technology) and rabbit anti-ERK1 mixed with rabbit anti-ERK2 antibody (both from Santa Cruz Biotechnology, USA). All primary antibodies were used at 1:1000 dilution. The secondary antibodies used were horseradish peroxidase-conjugated swine anti-rabbit or rabbit anti-mouse (Agilent, USA) diluted 1:3,000 in blocking solution. The control for protein loading was CoraLite® Plus 488-conjugated glyceraldehyde 3-phosphate dehydrogenase mouse monoclonal antibody (Proteintech) at 1:5,000.


https://doi.org/10.4048/jbc.2023.26.e47

### Migration assay

Cells in suspension were transfected in 96-well ImageLock microplates (Essen BioScience, USA). After 48 hours, the transfection medium was replaced with starvation medium and the cells were grown overnight. Wounds were created using an IncuCyte S3 96-pin Wound-Maker (Essen BioScience). After washing with PBS to remove detached cells, 100 μL of starvation medium was added to mitigate proliferation effects on migration. Alternatively, migration was induced by exposing cells to 50 ng/mL heregulinβ-1 (HRG-B1; Peprotech, UK), also referred to as neuregulin 1 or NRG1, in starvation medium. HRG serves as a ligand for HER3 and HER4 mainly by promoting HER2-HER3 heterodimerization [17,18]. An IncuCyte S3 (Essen BioScience) captured automated wound images at 12-hour intervals over 96 hours. IncuCyte™ software was used to analyze wound closure kinetics, with area under the curves used for comparison. Each sample was measured in triplicate and the experiment was repeated a minimum of three times.

### Transwell migration

To explore cell migratory responses affected by various siRNA treatments, we conducted transwell migration experiments using the IncuCyte Chemotaxis Assay with 8 μm pore membranes. Using a 10% FBS-containing medium, our goal was to examine direct migration towards a chemoattractant. After 48 hours of transfection, the cells were trypsinized and suspended in a starvation medium. They were then plated onto IncuCyte Clearview 96-well plates ($5 \times 10^6$ cells/well in 60 μL) in the upper chamber. In the lower chamber, 200 μL of 10% FBS-containing medium was added. Images were taken at 24-hour intervals over 96 hours, and the confluence area of cells on the membrane's bottom surface was normalized against the initial confluence on the top surface using IncuCyte™ software. Each sample was assayed in duplicate and the experiment was replicated three times.

### Proliferation

After 48 h of transfection with the siRNAs, the cells were trypsinized and plated in 96-well plates at 5%–10% confluence. The cells underwent cell proliferation analysis for 144 hours, with measurements taken at 24-hour intervals using an IncuCyte S3 high-content imager. Proliferation was quantified by assessing the confluence area normalized to that of the first scan (time point 0). Each sample was measured in six wells of a 96-well plate and the experiments were repeated a minimum of three times.

### HER2/ERBB2 transient overexpression

Human embryonic kidney 2 cells (HEK-239) were grown in DMEM containing 10% FBS, 5 mM ultraglutamine, and 100 U/mL penicillin-streptomycin. Cells were plated in 6-well plates and transfected with 3 μg of pEGFP empty vector or pERBB2-GFP (Addgene 39321) expression plasmid using FuGENE 6 (Promega, USA) following the manufacturer's protocol. After 48 hours of transfection, the cells were starved by serum deprivation for 24 hours and stimulated with medium containing 50% FBS for 30 minutes. The experiment was repeated three times.

### Statistics

Kaplan–Meier curves and their respective *p*-values were obtained from the KM Plotter portal. Spearman's correlation test was used to examine the correlation between *ERBB2* and formin mRNA expression. Student's *t*-test was used to assess differences in clinicopathological parameters and changes in cell migration and proliferation. $\chi^2$ test was used to analyze histological grade, formin staining scores, and lymph node metastasis frequencies. Statistical


https://doi.org/10.4048/jbc.2023.26.e47

analyses were performed using IBM SPSS Statistics version 26.0. Significance was defined as two-tailed *p* values ≤ 0.05.

## RESULTS

### High FHOD1, INF2, and DAAM1 mRNAs associate with poor prognosis and correlate with ERBB2 expression

First, we investigated the association between formins expression and outcomes of HER2-positive breast cancer. For this purpose, we used a publicly available database and Kaplan–Meier overall survival analysis was performed for 14 formin mRNAs (*GRID2IP* was not available). Our analysis revealed that increased mRNA levels of *FHOD1* (hazard ratio [HR], 1.63; $p = 0.012$), *INF2* (HR, 1.62; $p = 0.0079$), and *DAAM1* (HR, 1.56; $p = 0.02$) were associated with a negative prognosis (**Figure 1A**). Furthermore, we investigated the link between formins and *ERBB2* mRNA expression and found significant positive correlations with *FHOD1* (R = 0.161, $p = 0.015$), *INF2* (R = 0.248, $p < 0.001$), and *DAAM1* (R = 0.195, $p = 0.003$) (**Figure 1B**). These results show that high expressions of *FHOD1, INF2,* and *DAAM1* are associated with a poorer prognosis and correlate with *ERBB2* expression in HER2-positive breast

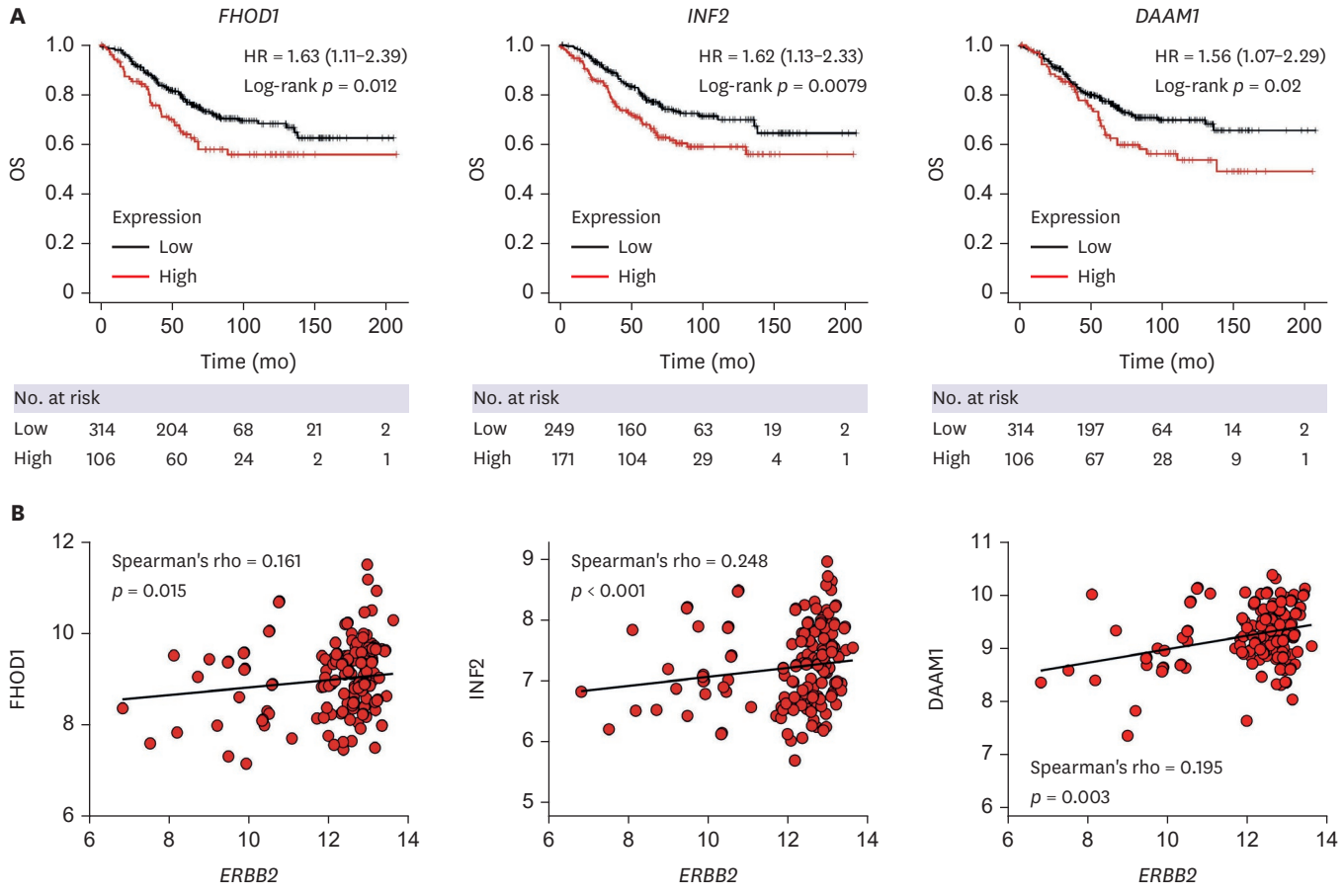


**Figure 1.** Kaplan–Meier overall survival and correlations between *ERBB2* and formin mRNA expression. (A) Kaplan–Meier OS analyses of HER2-positive breast cancer samples reveal significantly poorer prognosis associated with *FHOD1*, *INF2*, and *DAAM1* mRNA expression. The number of cases is denoted at the bottom of the figures. (B) *ERBB2* mRNA expression in HER2-positive subtype breast tumors (n = 230) exhibits a significant positive correlation with FHOD1, INF2, and DAAM1. Kaplan–Meier analyses and correlations for all formins, excluding GRIDIP, are depicted in **Supplementary Figures 1** and **2**. ERBB2 = erb-b2 receptor tyrosine kinase 2; HER2 = human epidermal growth factor receptor 2; OS = overall survival; HR = hazard ratio.


https://doi.org/10.4048/jbc.2023.26.e47

cancer. Kaplan–Meier plots and correlations for all formins (except *GRID2IP*) are shown in **Supplementary Figures 1** and **2**.

## IHC: higher FHOD1 expression correlates with lower ER and PgR positivity

Next, we validated FHOD1, INF2, and DAAM1 protein expression in TMAs comprising 70 HER2-positive breast cancer samples. Detailed clinicopathological attributes of the study cohort are shown in **Table 1**. The average age of the patients was 54.5 ± 9.2 years (range 32–70 years). Average tumor size was 21.7 ± 11.1 mm (range 5–70 mm). The proportions of Ki-67, ER, and PgR positivity were 34.5% ± 41.1% (range 5%–62%), 57.2% ± 41.1% (range 0%–95%), and 38.4% ± 37.4% (range 0%–98%), respectively. Approximately half of the patients exhibited lymph node metastasis. Tumor grading indicated that the majority (84.3%) were grade 3, 14.3% were grade 2, and 1.4% were grade 1.

Of the 70 patients, we acquired center and invasive border samples from 57 individuals, center samples from eight, and invasive border samples from five. The central and invasive border samples were merged for analysis because of their comparable staining results. The prevalent cytoplasmic staining intensity was scored as negative, low, moderate, or strong according to the scheme presented in **Figure 2**. No notable high-intensity INF2 was observed. For subsequent analysis, we grouped negative/low and moderate/strong for FHOD1, negative and low/moderate for INF2, and low and moderate/strong for DAAM1. Staining distribution exhibited greater homogeneity for FHOD1 and INF2 than for DAAM1. Specifically, DAAM1 displayed cytoplasmic granules in 34 tumors and, in six instances, a dual staining pattern with both cytoplasmic and membranous locations. Examples of DAAM1 staining patterns are shown in **Supplementary Figure 3**.

The correlations between FHOD1, INF2, and DAAM1 expression and clinicopathological features are shown in **Table 2**. A significant difference was observed in the average patient age with INF2 negative expressing tumors compared to INF2 low/moderate ($p = 0.004$). FHOD1 moderate/strong was associated with a lower percentage of ER ($p = 0.041$) and PgR ($p = 0.014$). Significantly higher values were observed for the percentages of Ki-67 ($p < 0.0001$) and lower values for ER ($p < 0.0001$) and PgR ($p < 0.002$) in grade 3 tumors than in grade 1/2 tumors (data not shown). All FHOD1 moderate/high samples were classified as grade 3. No significant differences in formin expression were observed in lymph node metastases.

**Table 1.** Clinicopathological characteristics of 70 HER2-subtype breast cancers used in the study

| Characteristics | Values |
|---|---|
| Age at surgery | 54.5 ± 9.2 (32–70) |
| Tumor diameter (mm) | 21.7 ± 11.1 (5–70) |
| Ki-67 (%) | 34.5 ± 41.1 (5–62) |
| ER (%) | 57.2 ± 41.1 (0–95) |
| PgR (%) | 38.4 ± 37.4 (0–98) |
| Lymph node metastasis | |
| Negative | 36 (51.4) |
| Positive | 34 (48.6) |
| Histological grade | |
| 1 | 1 (1.4) |
| 2 | 11 (14.3) |
| 3 | 65 (84.3) |

Values are presented as mean ± standard deviation (range) or number (%).
HER2 = human epidermal growth factor receptor 2; ER = estrogen receptor; PgR = progesterone receptor.


https://doi.org/10.4048/jbc.2023.26.e47

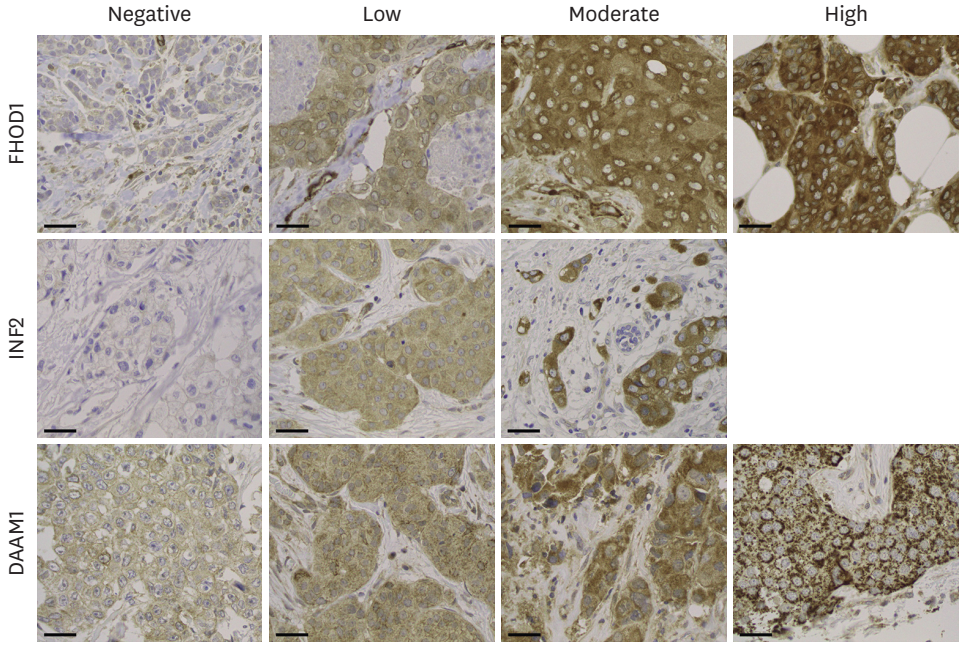


**Figure 2.** Immunohistochemistry. Tissue microarrays were sectioned at 3.5 μm and immunostained using FHOD1, INF2, or DAAM1 antibodies, following the streptavidin-peroxidase technique. The samples were evaluated based on the predominant staining intensity and categorized into four levels: negative, low, moderate, or strong. No instances of strong INF2 intensity were detected. Magnification: 400×. Scale bars = 50 μm.

**Table 2.** Correlation of FHOD1, INF2, and DAAM1 with clinicopathologic features

| Features | Age (yr) | Tumor size (mm) | Ki-67 (%) | ER (%) | PgR (%) | Lymph node metastasis | | Histological grade | |
|---|---|---|---|---|---|---|---|---|---|
| | | | | | | Negative | Positive | 1 + 2 | 3 |
| FHOD1 | | | | | | | | | |
| Negative/Low (n = 61) | 54.5 ± 9.2 (32–70) | 22.6 ± 11.4 (8–70) | 33.9 ± 11.9 (5–62) | 61.0 ± 31.1 (0–95) | 41.4 ± 38.5 (0–98) | 32 (52.5) | 29 (47.5) | 11 (18) | 50 (82) |
| Moderate/Strong (n = 9) | 54.2 ± 9.6 (40–60) | 25.3 ± 9.8 (5–39) | 38.4 ± 6.3 (30–55) | 31.1 ± 44.3 (0–90) | 17.8 ± 21.23 (0–85) | 4 (44.4) | 5 (55.6) | - | 9 (100) |
| p-value | 0.932 | 0.465 | 0.272 | 0.041 | 0.014 | 0.731 | | 0.336 | |
| INF2 | | | | | | | | | |
| Negative (n = 19) | 59.6 ± 7.2 (45–68) | 24.6 ± 9.6 (7–42) | 33.4 ± 12.8 (18–62) | 51.6 ± 44.4 (0–95) | 32.0 ± 39.7 (0–98) | 9 (47.4) | 10 (52.6) | 2 (10.5) | 17 (89.5) |
| Low/Moderate (n = 51) | 52.6 ± 9.2 (32–70) | 22.4 ± 11.7 (5–70) | 34.9 ± 11.0 (5–55) | 59.2 ± 40.1 (0–95) | 40.7 ± 36.7 (0–95) | 27 (52.9) | 24 (47.1) | 9 (17.7) | 42 (82.4) |
| p-value | 0.004 | 0.468 | 0.634 | 0.492 | 0.390 | 0.790 | | 0.715 | |
| DAAM1 | | | | | | | | | |
| Negative/Low (n = 54) | 54.4 ± 9.2 (38–70) | 22.70 ± 9.9 (7–42) | 34.1 ± 11.2 (13–62) | 54.6 ± 41.7 (0–95) | 39.0 ± 37.6 (0–98) | 29 (53.7) | 25 (46.3) | 9 (16.7) | 45 (83.3) |
| Moderate/Strong (n = 16) | 54.6 ± 9.7 (32–67) | 23.8 ± 14.9 (5–70) | 35.8 ± 12.7 (5–50) | 65.7 ± 39.3 (0–95) | 36.1 ± 38.0 (0–98) | 7 (43.8) | 9 (56.3) | 2 (12.5) | 14 (87.5) |
| p-value | 0.965 | 0.240 | 0.623 | 0.349 | 0.786 | 1 | | 1 | |

Values are presented as mean ± standard deviation (range) or number (%). ER = estrogen receptor; PgR = progesterone receptor.

## FHOD1, INF2, and DAAM1 influence migration in HER2/ERBB2-amplified breast cancer cells

For the cellular studies, two HER2-amplified breast cancer cell lines, MDA-MB-453 and SK-BR-3, were used. The subcellular localization of FHOD1, INF2, and DAAM1 in these breast cancer cell lines was studied using double immunofluorescence staining with phalloidin and anti-FHOD1 (**Figure 3**, upper panel), INF2 (middle panel), or DAAM1 (lower panel). Staining


https://doi.org/10.4048/jbc.2023.26.e47

revealed that these endogenous proteins were localized in the cytoplasm, mostly as small dots, in lamellipodia, and along actin filaments.

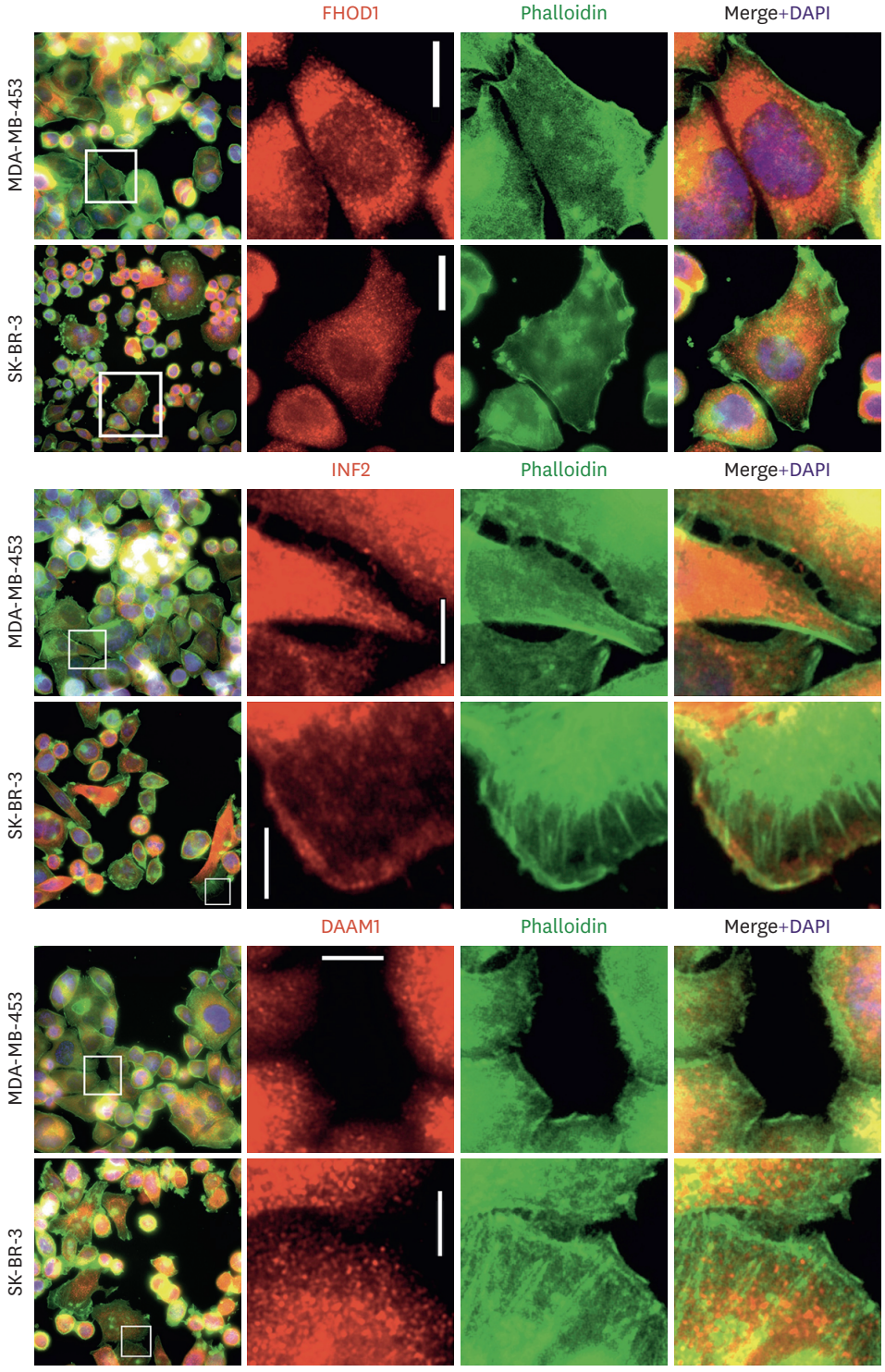


**Figure 3.** Localization of FHOD1, INF2, and DAAM1 in MDA-MB-453 and SK-BR-3 breast cancer cell lines. Upper panel: FHOD1 (red) is predominantly seen as cytoplasmic dots. Middle panel: INF2 (red) is distributed in the cytoplasm colocalized with phalloidin (green) and lamellipodia. Lower panel: DAAM1 (red) appears as cytoplasmic dots with co-localization with actin filaments. Magnification: 400×. Scale bars = 20 μm.


https://doi.org/10.4048/jbc.2023.26.e47

The functional roles of FHOD1, INF2, and DAAM1, both independently and in combination, were investigated in MDA-MB-453 and SK-BR-3 cells transfected with 50 nM siRNA specific to each formin or non-targeting control siRNA. The efficiency of the knockdown was evaluated 48-hour post-transfection by immunoblotting (**Figure 4A**). Despite siRNA-induced modulation, the cellular morphology, as shown in **Figure 4B**, remained unchanged.

To assess the knockdown effects of FHOD1, INF2, and DAAM1 on cell motility, we conducted wound-healing experiments. Starvation medium was used to minimize the influence of proliferation, and HRG was added to enhance the migration of slow-moving MDA-MB-453 and SK-BR-3 cells. In MDA-MB-453 cells, under both starvation and HRG conditions, FHOD1 ($p \leq 0.05$ and $p \leq 0.01$), FHOD1+INF2 ($p \leq 0.05$ and $p \leq 0.05$), FHOD1+DAAM1 ($p \leq 0.05$ and $p \leq 0.05$), and FHOD1+INF2+DAAM1 ($p \leq 0.05$ and $p \leq 0.05$) siRNAs delayed migration. In SK-BR-3 cells, significant siRNA effects were observed for FHOD1, INF2, DAAM1, and their combinations in both starvation (FHOD1, INF2, DAAM1, INF2+DAAM1, FHOD1+INF2+DAAM1: $p \leq 0.05$; FHOD1+DAAM1: $p \leq 0.01$) and HRG-supplemented starvation medium (FHOD1, DAAM1, FHOD1+INF2: $p \leq 0.01$; INF2, INF2+DAAM1: $p \leq 0.05$; FHOD1+INF2+DAAM1: $p \leq 0.05$; FHOD1+DAAM1: $p \leq 0.01$; FHOD1+INF2+DAAM1: $p$

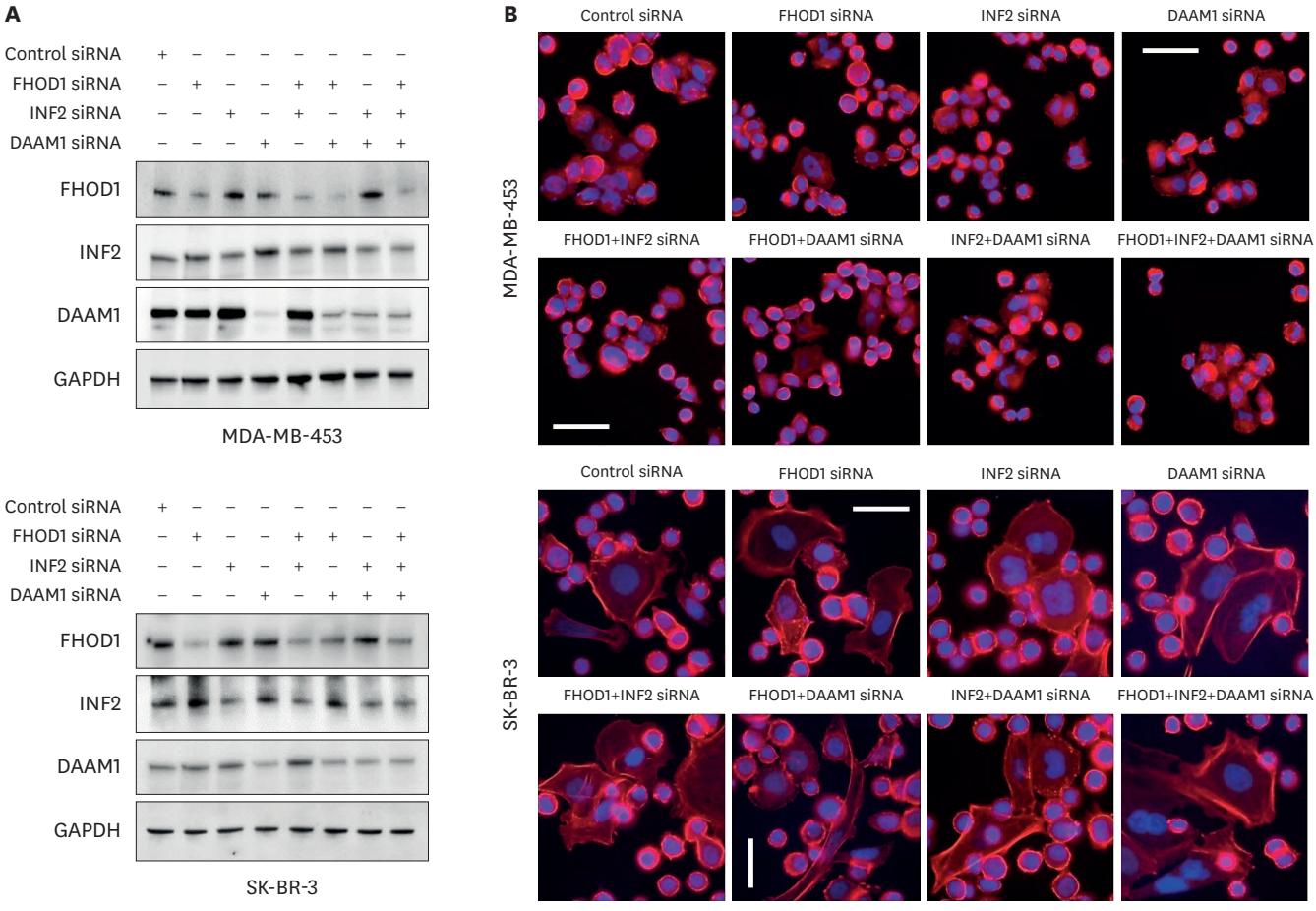


**Figure 4.** Small interfering RNA-mediated knockdown of FHOD1, INF2, DAAM1, or their combinations. (A) Knockdown effectiveness was assessed through immunoblotting 48-hour post-transfection, with GAPDH as a loading control. (B) Representative images of transfected cells with control, FHOD1, INF2, DAAM1, or combined siRNAs. Alexa Fluor 488-conjugated phalloidin and DAPI were used to visualize actin filaments and nuclei, respectively. Magnification: 400×. Scale bars = 50 μm. GAPDH = glyceraldehyde 3-phosphate dehydrogenase; siRNA = small interfering RNA; DAPI = 4′,6-diamidino-2-phenylindole.


https://doi.org/10.4048/jbc.2023.26.e47

≤ 0.001). Moreover, in SK-BR-3 cells, FHOD1+INF2+DAAM1 siRNAs showed an additional effect on HRG-induced migration (**Figure 5A**).

The transwell migration assay supported the wound healing results, showing heightened migration sensitivity. In MDA-MB-453 cells, reduction in all three formins simultaneously led to impaired migration over 72 hours ($p \leq 0.05$), whereas individual and combined siRNAs decreased migration at 96 hours (all $p \leq 0.05$). In SK-BR-3 cells, treatment with DAAM1 siRNA combined with FHOD1 ($p \leq 0.01$), INF2 ($p \leq 0.001$), or both ($p \leq 0.001$) impaired cell migration at 48 hours. At 72-hour, all individual siRNAs and their combinations led to diminished migration (FHOD1, $p \leq 0.05$; INF2 and DAAM1, $p \leq 0.01$; FHOD1+INF2, $p \leq 0.05$; FHOD1+DAAM1, $p \leq 0.01$; INF2+DAAM1; and FHOD1+INF2+DAAM1, $p \leq 0.001$). By 96-hour, significant effects were observed for INF2, DAAM1, FHOD1+DAAM1, and INF2+DAAM1 ($p \leq 0.05$), and for FHOD1+INF2 and FHOD1+INF2+DAAM1 ($p \leq 0.01$) (**Figure 5B**).

## Proliferation was impacted when FHOD1, INF2, and DAAM1 were simultaneously knocked down

Proliferation was assessed by quantifying the cell area over a 144-hour period. A significant reduction in the proliferation of MDA-MB-453 cells was observed only when all three formins (FHOD1, INF2, and DAAM1) were simultaneously downregulated ($p \leq 0.05$) (**Figure 5C**).

## HER2/ERBB2 knockdown resulted in reduced expression of FHOD1 and INF2 via the Akt and MAPK pathways

Immunostaining using a specific HER2 antibody on MDA-MB-453 and SK-BR-3 cells revealed HER2 localization in both the nucleus and cytoplasm, with concentrations in the actin-rich cellular protrusions (**Figure 6A**).

To explore the influence of HER2 downstream pathways on FHOD1, INF2, and DAAM1 expression, cells were transfected with an *ERBB2*-targeting siRNA. Knockdown efficiency was verified by western blotting in both the MDA-MB-453 and SK-BR-3 cell lines (**Figure 6B**).

Subsequently, we investigated FHOD1, INF2, and DAAM1 expression dependency on the individual MAPK or PI3K signaling pathways. MDA-MB-453 and SK-BR-3 cells were exposed to the MEK1/2 inhibitor UO126, the PI3 kinase inhibitor LY294002, or the control vehicle DMSO. Effective pathway inhibition was corroborated by western blot analysis of Akt and MAPK phosphorylation (**Figure 6B**).

Upon HER2/ERBB2 knockdown, MDA-MB-453 cells displayed decreased levels of FHOD1, INF2, and DAAM1, along with reduced phosphorylated MAPK (pMAPK) levels. Treatment with PI3K or MAPK inhibitors replicated the effects observed with HER2/ERBB2 knockdown, thereby confirming the regulatory influence of ERBB2 on FHOD1 and INF2 expression through the Akt/MAPK pathway in this cell line. Notably, while ERBB2 knockdown affected DAAM1 expression, the individual inhibition of the PI3K or MAPK pathways did not elicit similar changes.

In SK-BR-3 cells, ERBB2 knockdown decreased FHOD1 and INF2 levels and reduced Akt/pAkt and MAPK phosphorylation. However, inhibition of either PI3K or MAPK alone did not induce changes in the expression of these formins. These results underline the impact of HER2 on the Akt/MAPK pathways, suggesting that the activation of both pathways is either necessary for or contributes to the regulation of FHOD1 and INF2 expression. The DAAM1


https://doi.org/10.4048/jbc.2023.26.e47

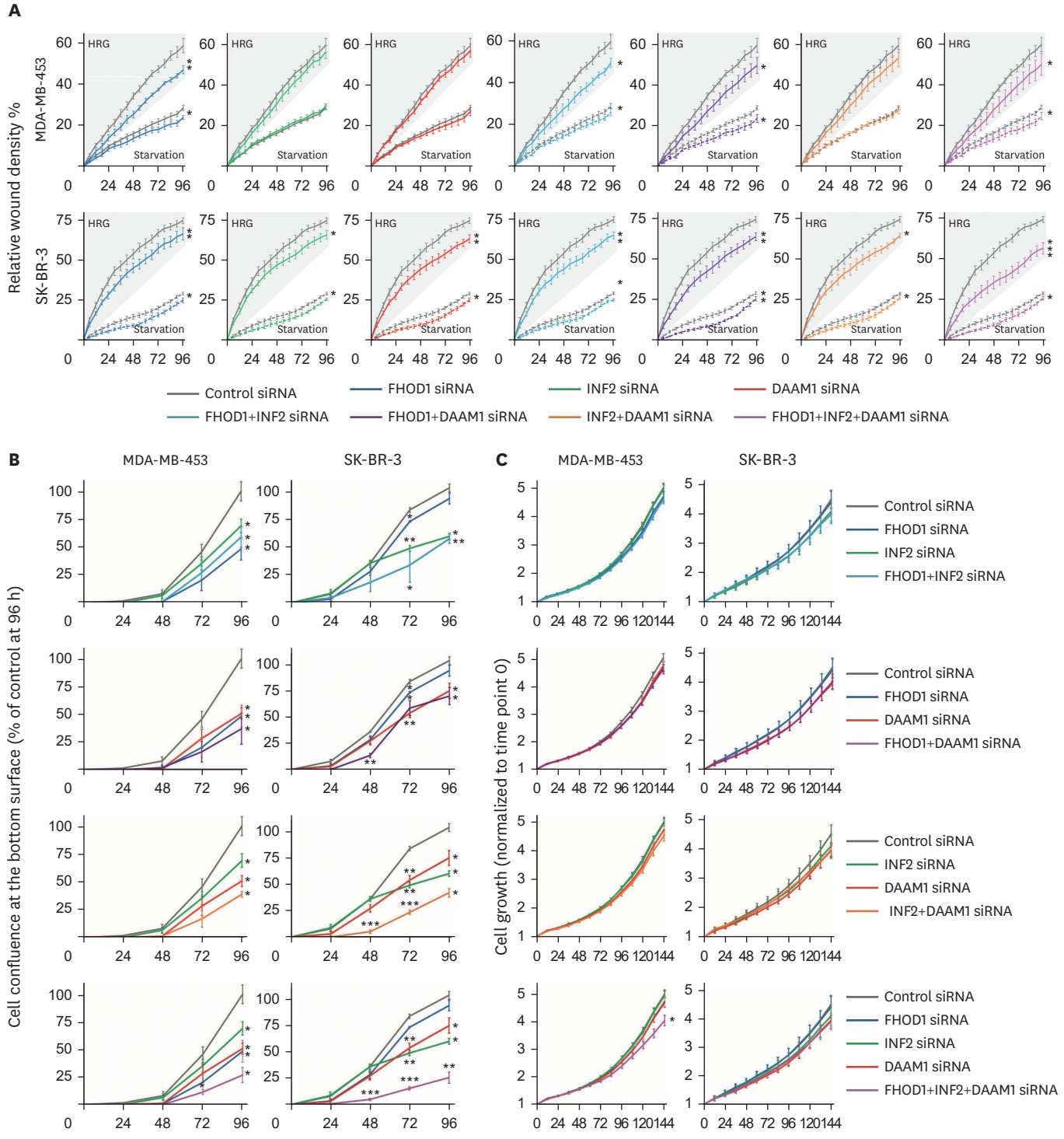


**Figure 5.** Effect of knockdown of FHOD1, INF2, DAAM1 or their combination in wound healing, transwell migration, and proliferation. (A) Scratch wounds were performed 48-hour post siRNA transfection, and the medium subsequently replaced by starvation medium or starvation medium supplemented with 50 ng/mL HRG to speed migration. The wound relative densities were monitored over 96 hours. (B) Forty-eight hours after transfection, cells were seeded on the upper surface of the transwell migration chamber, while the lower chamber contained medium supplemented with 10% serum as a chemoattractant. Confluence of cells on the bottom surface of the membrane was monitored for 96 h and normalized based on the initial top surface cell area for each well. (C) For proliferation assessment, cells were plated to cover 5%–10% of the area 48-hour post-transfection, and the growth of confluence measured over 144 hours. Comparisons between cells treated with control siRNA and those subjected to FHOD1, INF2, DAAM1, and their combinations were analyzed using Student's *t*-test, where $^{*}p \leq 0.05$, $^{**}p \leq 0.01$, and $^{***}p \leq 0.001$ were considered statistically significant.
siRNA = small interfering RNA; HRG = heregulin.


https://doi.org/10.4048/jbc.2023.26.e47

Journal of Breast Cancer JBC

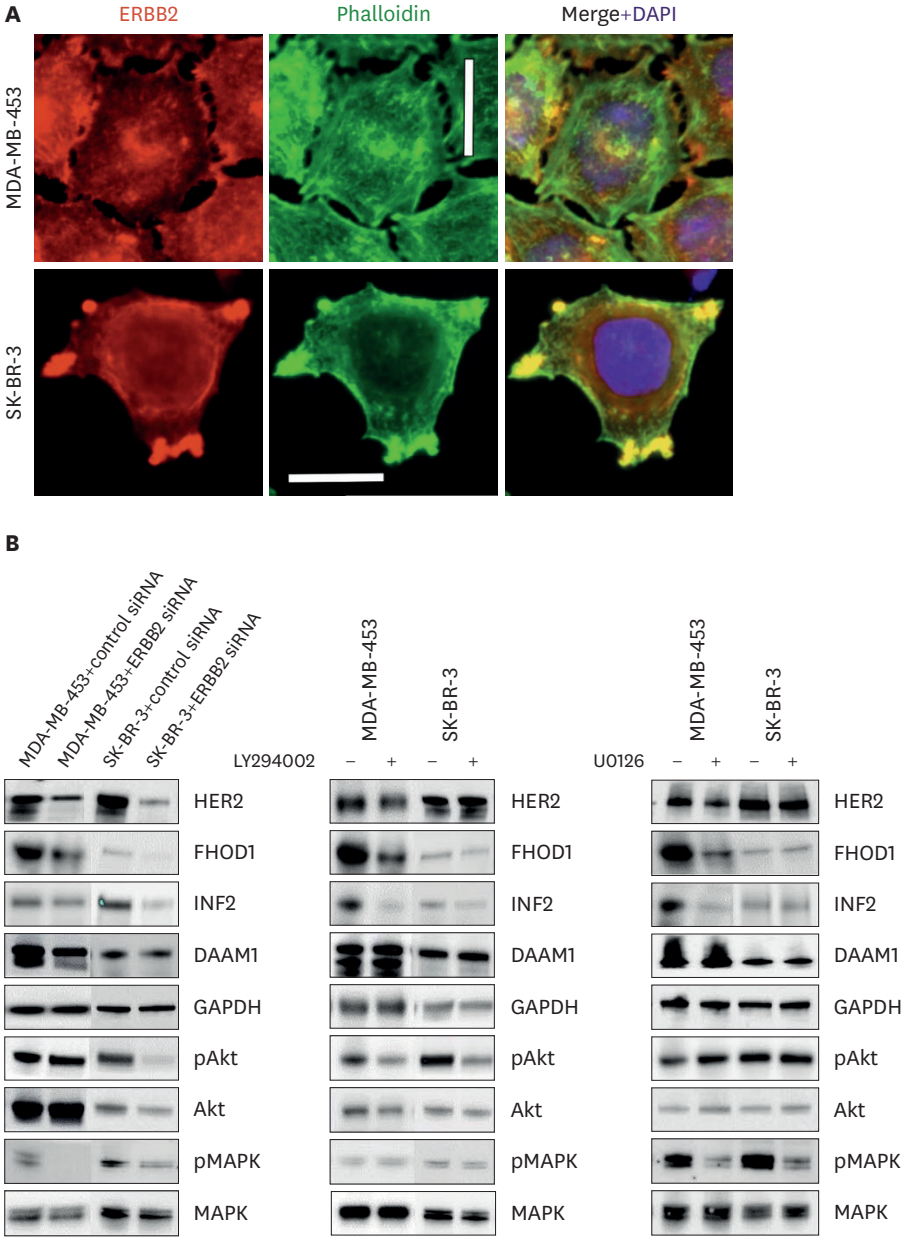


**Figure 6.** HER2/ERBB2 knockdown alters FHOD1 and INF2 expression through Akt and MAPK pathways. (A) Subcellular localization of HER2 (in red) in MDA-MB-453 and SK-BR-3 cells, with ERBB2 concentrated in actin-rich cellular protrusions, observed through phalloidin staining (green). DAPI (blue) indicates nuclei. Magnification: 400×. Scale bars = 20 μm. (B) Cells were treated with ERBB2 siRNA for 48 hours, and the knockdown efficacy validated by western blotting in both MDA-MB-453 and SK-BR-3 cells. In MDA-MB-453 cells, HER2/ERBB2 knockdown decreased FHOD1, INF2, and DAAM1 levels, concomitant with a reduction in pMAPK. In SK-BR-3 cells, ERBB2 knockdown reduced FHOD1 and INF2 expression, accompanied by lowered Akt/pAkt and MAPK phosphorylation levels. Both cell lines were treated with MEK1/2 inhibitor UO126, PI3K inhibitor LY294002, or the control vehicle DMSO. Effective pathway inhibition was verified by western blotting of Akt and MAPK phosphorylation states. Treatment with PI3K or MAPK inhibitors in MDA-MB-453 cells emulated the effects of HER2/ERBB2 knockdown, decreasing FHOD1 and INF2 expression. In contrast, inhibiting PI3K or MAPK alone did not induce alterations in FHOD1 and INF2 levels in SK-BR-3 cells. Notably, DAAM1 levels remained unaffected by PI3K or MAPK inhibitor treatments in both cell lines. HER2 = human epidermal growth factor receptor 2; ERBB2 = erb-b2 receptor tyrosine kinase 2; DAPI = 4′,6-diamidino-2-phenylindole; siRNA = small interfering RNA.

results were less conclusive, suggesting different pathways. Exogenous ERBB2 overexpression in HEK-239 cells did not affect the expression of FHOD1, INF2, or DAAM1 (**Supplementary Figure 4**).


https://doi.org/10.4048/jbc.2023.26.e47

## DISCUSSION

The formin protein family consists of 15 members, many of which have been shown to play crucial roles in the progression of various cancers, and are interconnected via the same signaling pathways as HER2. In this study, we provide evidence that, at the mRNA level, three specific formins are correlated with outcomes in HER2-positive breast cancer and are associated with *ERBB2* in the HER2-subtype of breast cancer. Moreover, increased FHOD1 expression in tumor samples was linked to a higher histological grade and exhibited a negative correlation with ER and PgR percentages. Our *in vitro* investigations revealed that the knockdown of formins results in reduced migration. Importantly, we revealed that HER2 can regulate the expression of FHOD1, INF2, and DAAM1. Recognizing formins as components of the HER2 knockdown response holds potential significance for identifying drug targets for the treatment of HER2-subtype breast cancer.

Using publicly accessible online tools, we identified a correlation between formin expression and *ERBB2* mRNA levels along with their prognostic implications for HER2-subtype breast cancer. It is worth noting that mRNA quantification is predominantly based on averaging across all cell types present in the tissue, which might disregard intratumoral heterogeneity. Consequently, we aimed to ascertain whether a comparable correlation could be established at the protein level, specifically within cancer cells, using IHC. Unfortunately, possibly due to the limited sample size, we were unable to ascertain such a correlation. However, our observations revealed a connection between low ER and PgR percentages and an elevated tumor grade. These findings align with the outcomes observed in a cohort of 450 patients with HER2-positive breast cancer, in which the absence of receptor expression correlated with a higher histological grade and independently predicted unfavorable disease-free survival [19].

In our investigation, we observed a notable trend wherein all samples expressing FHOD1 at moderate to high levels were characterized by histologic grade 3. Additionally, we identified a negative correlation between elevated FHOD1 expression and reduced ER and PgR percentages, implying a potential link between FHOD1 upregulation and tumor dedifferentiation. This suggests that FHOD1 may be elevated in tandem with tumor dedifferentiation. Numerous studies have posited that cell dedifferentiation can coincide with epithelial-mesenchymal transition (EMT) [20-22]. The role of FHOD1 in this context has been elucidated, with its overexpression observed during EMT. This is often accompanied by the upregulation of EMT markers such as N-cadherin, vimentin, and collagen, along with the downregulation of epithelial markers including E-cadherin, keratins, integrins, and laminins, as reported in squamous cell carcinoma [12].

We used HER2-amplified cell lines to perform siRNA-mediated knockdown experiments targeting formins to uncover their impact on migration and proliferation. Our findings revealed that the depletion of FHOD1, INF2, or DAAM1, either individually or in combination, led to a deceleration in the migration of SK-BR-3 cells under both starvation and HRG-B1 stimulation. Notably, an additional effect was observed when all the three formins were concurrently knocked down. In MDA-MB-453 cells, which exhibited a relatively slower migration profile than SK-BR-3 cells, a notable delay in migration manifested exclusively upon knockdown of FHOD1, DAAM1, or their combination. These results are in line with those of recent studies in the field of breast cancer research, which have shown the impact of various formins, including FHOD1, INF2 [10], FMNL2 [23], DAAM1 [24-26], and FMNL1 [7].


https://doi.org/10.4048/jbc.2023.26.e47

Transwell migration experiments confirmed these effects, showing enhanced outcomes with the combination of siRNAs targeting specific formins. The dynamic actin cytoskeleton forms actin clouds, providing mechanical support, force generation, and cellular adaptability, with the nuclei acting as mechanosensors, as previously shown [27,28]. Particularly noteworthy was the enhanced effect observed when DAAM1 siRNA was present in MDA-MB-453 cells and INF2 siRNA was present in SK-BR-3 cells. These findings underscore the cell-specific nature of formin migration. In terms of proliferation, we observed a slight decrease when FHOD1, INF2, and DAAM1 were concurrently depleted in MDA-MB-453 cells. Consistently, several published studies have reported the impact of formins on cell proliferation [29-31], which may arise from their involvement in diverse processes such as cytokinesis [32], microtubule stabilization [33,34], and modulation of the cell cycle through activation of the serum response element [9,35].

Because of the positive correlation observed between *ERBB2* mRNA levels and *FHOD1, INF2, and DAAM1* mRNA levels in tumor samples, the key objective of this study was to explore whether HER2/ERBB2 downstream signaling plays a role in regulating the expression of these formins *in vitro*. Our investigations using MDA-MB-453 and SK-BR-3 cells validated this hypothesis. Specifically, we demonstrated that a reduction in HER2/ERBB2 expression resulted in decreased FHOD1 and INF2 expression in both cell lines. Moreover, in SK-BR-3 cells, this knockdown led to a reduction in the phosphorylation of Akt and MAPK, whereas in MDA-MB-453 cells, only the MAPK pathway was affected. These findings emphasize the involvement of ERBB2-mediated signaling cascades in the modulation of FHOD1 and INF2 expression, highlighting their potential significance in breast cancer pathobiology. Emerging research has provided further support for the interplay between HER2/ERBB2 signaling and formin expression. In a study involving the high HER2/ERBB2-expressing cell line BT-474, treatment with trastuzumab, which is known to inhibit HER2 activation, yielded significant reductions in *FHOD1* and *INF2* mRNA levels (both exhibiting a 1.56-fold decrease). Notably, this decrease was accompanied by downregulation of the proliferative marker Ki-67 [36], underscoring the potential impact of HER2/ERBB2 modulation on the expression of these formins and subsequent cellular processes, such as proliferation. In another study involving SK-BR-3 cells treated with lapatinib, an inhibitor targeting ERBB1/EGFR and HER2 phosphorylation, the protein levels of INF2 underwent significant reduction (1.63-fold) [37]. Consistent with these findings, our experimental results aligned with the observed effects on INF2 and FHOD1 expression following *ERBB2* siRNA-mediated knockdown in both SK-BR-3 and MDA-MB-453 cell lines. This knockdown was accompanied by a reduction in Akt and MAPK phosphorylation in SK-BR-3 cells, while in MDA-MB-453 cells, only MAPK phosphorylation levels were decreased. Importantly, our study outcomes are in line with those of previous research from our own group, which demonstrated the regulatory influence of the PI3K-Akt and RAS-MAPK pathways on formin expression in squamous cell carcinoma [12] and melanoma [8].

Our inhibitor experiments revealed distinct regulatory mechanisms in the MDA-MB-453 and SK-BR-3 cells. In MDA-MB-453 cells, the inhibition of PI3K or MAPK replicated the FHOD1 and INF2 reductions observed after ERBB2 knockdown, indicating their regulation through these pathways. In SK-BR-3 cells, downregulation of both pAkt and pMAPK was necessary for changes in FHOD1 and INF2 expression. This is consistent with the suggestion that combining PI3K or MEK inhibition with anti-HER2 therapy could enhance the treatment of patients with HER2-positive gastric cancer [38]. However, the connection between HER2/ERBB2 knockdown and DAAM1 expression remains inconclusive. Although ERBB2 knockdown led to a slight decrease in DAAM1 expression in MDA-MB-453 cells, accompanied by reduced pMAPK levels, this relationship was not confirmed when using a

MAPK-specific inhibitor. This suggests that another pathway downstream of HER2/ERBB2 regulates DAAM1. Unlike FHOD1, which remains inactive until it is bound by Rho GTPases [39], and INF2, which lacks direct regulation [40], DAAM1 interacts with DVL (DVL-DAAM1) to activate RHO or RAC GTPases. This triggers JNK and ROCK activation, culminating in cytoskeletal rearrangement in response to Wnt stimulation.

Although many patients with ERBB2-positive metastatic breast cancer initially respond to trastuzumab-based therapies, resistance often develops. Activation of the PI3K pathway has been identified as a key factor in trastuzumab resistance, along with alterations in the downstream components of the PI3K/Akt signaling pathway [41] or target downstream components. The search for alternative therapeutic targets related to HER2 may provide a strategy for overcoming this resistance. Our study highlighted FHOD1 and INF2 as downstream effectors of the HER2/Akt and HER2/MAPK pathways, making them potential candidates for future therapeutic interventions. An encouraging compound, SMIFH2, has been shown to disrupt specific actin structures regulated by formins, resulting in antiproliferative effects by affecting cell division and motility [42]. However, recent findings suggest that SMIFH2 may also inhibit certain classes of myosins, along with formins [43], prompting ongoing efforts to discover more specific antiformin drugs.

## ACKNOWLEDGEMENTS

We thank James Conway for kindly providing us with the perbB2-GFP vector, Pauliina Munne for her role in the acquisition of tumor samples, and Deepankar Chakroborty and Majid Momeny for their support, contribution, and/or suggestions during this study.

## SUPPLEMENTARY MATERIALS

### Supplementary Table 1

Cutoff values and probes used for Kaplan–Meier overall survival analyses

Click here to view

### Supplementary Figure 1

Kaplan–Meier plots obtained from all formins (except GRID2IP).

Click here to view

### Supplementary Figure 2

Correlations between formins and *ERBB2* mRNA in 230 HER2-positive subtype breast tumors (not available for GRIDIP).

Click here to view

### Supplementary Figure 3

DAAM1 staining patterns.

Click here to view

**Supplementary Figure 4**

HEK-239 cells were transfected with EGFP or ERBB2-EGFP. Transfection efficiency was confirmed by western blot 48 hours after transfection. Serum stimulation for 30 minutes heightened pAkt levels in both EGFP and EGFP-ERBB2 transfected cells but had no significant impact on pMAPK phosphorylation or the expression of FHOD1, INF2, and DAAM1.

Click here to view

## REFERENCES

1. Sung H, Ferlay J, Siegel RL, Laversanne M, Soerjomataram I, Jemal A, et al. Global cancer statistics 2020: GLOBOCAN estimates of incidence and mortality worldwide for 36 cancers in 185 countries. CA Cancer J Clin 2021;71:209-49.
PUBMED | CROSSREF
2. WHO. Breast Tumours. WHO Classification of Tumours. 5th ed. Geneva: WHO Classification Editorial Board; 2019.
3. Holbro T, Beerli RR, Maurer F, Koziczak M, Barbas CF 3rd, Hynes NE. The ErbB2/ErbB3 heterodimer functions as an oncogenic unit: ErbB2 requires ErbB3 to drive breast tumor cell proliferation. Proc Natl Acad Sci U S A 2003;100:8933-8.
PUBMED | CROSSREF
4. Sirkisoon SR, Carpenter RL, Rimkus T, Miller L, Metheny-Barlow L, Lo HW. EGFR and HER2 signaling in breast cancer brain metastasis. Front Biosci (Elite Ed) 2016;8:245-63.
PUBMED | CROSSREF
5. Tiwari RK, Borgen PI, Wong GY, Cordon-Cardo C, Osborne MP. HER-2/neu amplification and overexpression in primary human breast cancer is associated with early metastasis. Anticancer Res 1992;12:419-25.
PUBMED
6. Schönichen A, Geyer M. Fifteen formins for an actin filament: a molecular view on the regulation of human formins. Biochim Biophys Acta 2010;1803:152-63.
PUBMED | CROSSREF
7. Favaro P, Traina F, Machado-Neto JA, Lazarini M, Lopes MR, Pereira JK, et al. FMNL1 promotes proliferation and migration of leukemia cells. J Leukoc Biol 2013;94:503-12.
PUBMED | CROSSREF
8. Gardberg M, Heuser VD, Koskivuo I, Koivisto M, Carpen O. FMNL2/FMNL3 formins are linked with oncogenic pathways and predict melanoma outcome. J Pathol Clin Res 2016;2:41-52.
PUBMED | CROSSREF
9. Peippo M, Gardberg M, Lamminen T, Kaipio K, Carpén O, Heuser VD. FHOD1 formin is upregulated in melanomas and modifies proliferation and tumor growth. Exp Cell Res 2017.350:267-78.
PUBMED | CROSSREF
10. Heuser VD, Mansuri N, Mogg J, Kurki S, Repo H, Kronqvist P, et al. Formin proteins FHOD1 and INF2 in triple-negative breast cancer: association with basal markers and functional activities. Breast Cancer (Auckl) 2018;12:1178223418792247.
PUBMED | CROSSREF
11. Yang XY, Liao JJ, Xue WR. FMNL1 down-regulation suppresses bone metastasis through reducing TGF-β1 expression in non-small cell lung cancer (NSCLC). Biomed Pharmacother 2019;117:109126.
PUBMED | CROSSREF
12. Gardberg M, Kaipio K, Lehtinen L, Mikkonen P, Heuser VD, Talvinen K, et al. FHOD1, a formin upregulated in epithelial-mesenchymal transition, participates in cancer cell migration and invasion. PLoS One 2013;8:e74923.
PUBMED | CROSSREF
13. Zhong B, Wang K, Xu H, Kong F. Silencing Formin-like 2 inhibits growth and metastasis of gastric cancer cells through suppressing internalization of integrins. Cancer Cell Int 2018;18:79.
PUBMED | CROSSREF
14. Rong Y, Gao J, Kuang T, Chen J, Li JA, Huang Y, et al. DIAPH3 promotes pancreatic cancer progression by activating selenoprotein TrxR1-mediated antioxidant effects. J Cell Mol Med 2021;25:2163-75.
PUBMED | CROSSREF

15. Győrffy B, Lanczky A, Eklund AC, Denkert C, Budczies J, Li Q, et al. An online survival analysis tool to rapidly assess the effect of 22,277 genes on breast cancer prognosis using microarray data of 1,809 patients. Breast Cancer Res Treat 2010;123:725-31.
PUBMED | CROSSREF

16. Park SJ, Yoon BH, Kim SK, Kim SY. GENT2: an updated gene expression database for normal and tumor tissues. BMC Med Genomics 2019;12 Suppl 5:101.
PUBMED | CROSSREF

17. Wallasch C, Weiss FU, Niederfellner G, Jallal B, Issing W, Ullrich A. Heregulin-dependent regulation of HER2/neu oncogenic signaling by heterodimerization with HER3. EMBO J 1995;14:4267-75.
PUBMED | CROSSREF

18. Graus-Porta D, Beerli RR, Daly JM, Hynes NE. ErbB-2, the preferred heterodimerization partner of all ErbB receptors, is a mediator of lateral signaling. EMBO J 1997;16:1647-55.
PUBMED | CROSSREF

19. Lee HJ, Park IA, Park SY, Seo AN, Lim B, Chai Y, et al. Two histopathologically different diseases: hormone receptor-positive and hormone receptor-negative tumors in HER2-positive breast cancer. Breast Cancer Res Treat 2014;145:615-23.
PUBMED | CROSSREF

20. Forte E, Chimenti I, Rosa P, Angelini F, Pagano F, Calogero A, et al. EMT/MET at the crossroad of stemness, regeneration and oncogenesis: the Ying-Yang equilibrium recapitulated in cell spheroids. Cancers (Basel) 2017;9:98.
PUBMED | CROSSREF

21. Jolly MK, Jia D, Boareto M, Mani SA, Pienta KJ, Ben-Jacob E, et al. Coupling the modules of EMT and stemness: a tunable 'stemness window' model. Oncotarget 2015;6:25161-74.
PUBMED | CROSSREF

22. Thiery JP, Acloque H, Huang RY, Nieto MA. Epithelial-mesenchymal transitions in development and disease. Cell 2009;139:871-90.
PUBMED | CROSSREF

23. Jiao X, Wang B, Yang L, Zhao Q, Zhang M, Liu X, et al. FMNL2 suppresses cell migration and invasion of breast cancer: a reduction of cytoplasmic p27 via RhoA/LIMK/Cofilin pathway. Cell Death Dis 2022;8:155.
PUBMED | CROSSREF

24. Dai B, Shen Y, Yan T, Zhang A. Wnt5a/ROR1 activates DAAM1 and promotes the migration in osteosarcoma cells. Oncol Rep 2020;43:601-8.
PUBMED

25. Hao L, Liu Y, Yu X, Zhu Y, Zhu Y. Formin homology domains of Daam1 bind to Fascin and collaboratively promote pseudopodia formation and cell migration in breast cancer. Cell Prolif 2021;54:e12994.
PUBMED | CROSSREF

26. Mei J, Xu B, Hao L, Xiao Z, Liu Y, Yan T, et al. Overexpressed DAAM1 correlates with metastasis and predicts poor prognosis in breast cancer. Pathol Res Pract 2020;216:152736.
PUBMED | CROSSREF

27. Lomakin AJ, Cattin CJ, Cuvelier D, Alraies Z, Molina M, Nader GP, et al. The nucleus acts as a ruler tailoring cell responses to spatial constraints. Science 2020;370:370.
PUBMED

28. Venturini V, Pezzano F, Català Castro F, Häkkinen HM, Jiménez-Delgado S, Colomer-Rosell M, et al. The nucleus measures shape changes for cellular proprioception to control dynamic cell behavior. Science 2020;370:370.
PUBMED

29. Jiao X, Wang B, Feng C, Song S, Tian B, Zhou C, et al. Formin-like protein 2 promotes cell proliferation by a p27-related mechanism in human breast cancer cells. BMC Cancer 2021;21:760.
PUBMED | CROSSREF

30. Zhang Z, Dai F, Luo F, Wu W, Zhang S, Zhou R, et al. Diaphanous related formin 3 knockdown suppresses cell proliferation and metastasis of osteosarcoma cells. Discov Oncol 2021;12:20.
PUBMED | CROSSREF

31. Hu J, Lu J, Lian G, Ferland RJ, Dettenhofer M, Sheen VL. Formin 1 and filamin B physically interact to coordinate chondrocyte proliferation and differentiation in the growth plate. Hum Mol Genet 2014;23:4663-73.
PUBMED | CROSSREF

32. Bohnert KA, Willet AH, Kovar DR, Gould KL. Formin-based control of the actin cytoskeleton during cytokinesis. Biochem Soc Trans 2013;41:1750-4.
PUBMED | CROSSREF

33. DeWard AD, Eisenmann KM, Matheson SF, Alberts AS. The role of formins in human disease. Biochim Biophys Acta 2010;1803:226-33.
PUBMED | CROSSREF

34. Bartolini F, Gundersen GG. Formins and microtubules. Biochim Biophys Acta 2010;1803:164-73.
PUBMED | CROSSREF

35. Jurmeister S, Baumann M, Balwierz A, Keklikoglou I, Ward A, Uhlmann S, et al. MicroRNA-200c represses migration and invasion of breast cancer cells by targeting actin-regulatory proteins FHOD1 and PPM1F. Mol Cell Biol 2012;32:633-51.
PUBMED | CROSSREF

36. von der Heyde S, Wagner S, Czerny A, Nietert M, Ludewig F, Salinas-Riester G, et al. mRNA profiling reveals determinants of trastuzumab efficiency in HER2-positive breast cancer. PLoS One 2015;10:e0117818.
PUBMED

37. O'Connell K, Li J, Engler F, Hennessy K, O'Neill F, Straubinger RM, et al. Determination of the Proteomic Response to Lapatinib Treatment using a comprehensive and reproducible ion-current-based proteomics strategy. J Proteom Genom Res 2013;1:27-42.
PUBMED | CROSSREF

38. Mezynski MJ, Farrelly AM, Cremona M, Carr A, Morgan C, Workman J, et al. Targeting the PI3K and MAPK pathways to improve response to HER2-targeted therapies in HER2-positive gastric cancer. J Transl Med 2021;19:184.
PUBMED | CROSSREF

39. Takeya R, Taniguchi K, Narumiya S, Sumimoto H. The mammalian formin FHOD1 is activated through phosphorylation by ROCK and mediates thrombin-induced stress fibre formation in endothelial cells. EMBO J 2008;27:618-28.
PUBMED | CROSSREF

40. Hegsted A, Yingling CV, Pruyne D. Inverted formins: a subfamily of atypical formins. Cytoskeleton (Hoboken) 2017;74:405-19.
PUBMED | CROSSREF

41. Saal LH, Holm K, Maurer M, Memeo L, Su T, Wang X, et al. PIK3CA mutations correlate with hormone receptors, node metastasis, and ERBB2, and are mutually exclusive with PTEN loss in human breast carcinoma. Cancer Res 2005;65:2554-9.
PUBMED | CROSSREF

42. Rizvi SA, Neidt EM, Cui J, Feiger Z, Skau CT, Gardel ML, et al. Identification and characterization of a small molecule inhibitor of formin-mediated actin assembly. Chem Biol 2009;16:1158-68.
PUBMED | CROSSREF

43. Nishimura Y, Shi S, Zhang F, Liu R, Takagi Y, Bershadsky AD, et al. The formin inhibitor SMIFH2 inhibits members of the myosin superfamily. J Cell Sci 2021;134:134.
PUBMED | CROSSREF